and **3A**, to a value much shorter than a typical Si–Si bond, as the compounds strive to maintain their strong Si–O bonds. The strain engendered by two bridging oxygens overwhelms the possibility of Si–Si bonding in the biradicals **2B** and **2B'**. If there are three bridges as in **3B** the silicons are held at a bonding distance, but inspection of the orbitals shows **3B** is also a biradical. Thus experimental isolation of **2B**, **2B'**, or **3B** seems unlikely.

It is important to use the appropriate level of electronic structure theory to describe these compounds. RHF calculations on **2B** are completely misleading, while the use of RHF calculations for singlet **3B** does not correctly predict the multiplicity of the ground state. The availability of analytically computed TCSCF energy second derivatives, necessary to verify the existence of minima on a potential energy surface, is a key component of these calculations.

Nature of the Transition Structure for Oxygen Atom Transfer from a Hydroperoxide. Theoretical Comparison between Water Oxide and Ammonia Oxide

Robert D. Bach,[*,†] **Amy L. Owensby,**[†] **Carlos Gonzalez,**[†] **H. Bernhard Schlegel,**[†] and **Joseph J. W. McDouall**[‡]

Contribution from the Departments of Chemistry, Wayne State University, Detroit, Michigan 48202, and University of Manchester, Manchester M13 9PL, U.K. Received November 26, 1990

Abstract: A theoretical study of the mechanism of oxygen atom transfer from hydrogen peroxide and an alkyl hydrogen peroxide is described. Ab initio molecular orbital calculations were carried out with the 6-31G* basis set (and larger basis sets for selected reactions). All key equilibrium geometries and transition states were optimized at the MP2 level; barriers were calculated at the MP4SDTQ level with use of the MP2 optimized geometry. The barrier for HOOH → H₂OO is ca. 54 kcal/mol. The reverse reaction, H₂OO → HOOH, shows no barrier at the MP4 level when the HF optimized geometries are used, but it does have a barrier of 3.9 or 3.7 kcal/mol when the geometry is optimized at the MP2 or MP4 level, respectively. By contrast, a comparatively high barrier (27 kcal/mol) is found for H₃NO → H₂NOH, which is relatively insensitive to correlation effects on the geometry. The oxidation of ammonia by hydrogen peroxide is shown to be a 2-step process dominated by a 1,2-hydrogen shift (54-kcal/mol barrier) followed by a facile S_N2-like displacement (2-kcal/mol barrier) to afford H₃NO + H₂O. The active bonds in the transition state are generally shorter when optimized at the MP2, CASSCF, CISD, and QCISD levels than at the HF level. All four levels agree that the barrier for oxygen transfer from water oxide is very low. The NH₃ + H₂O₂ reaction has been compared to the two identity reactions, H₂O + H₂O₂ and NH₃ + H₃NO, and an orbital interaction picture has been developed to explain the differences. The high barrier for the 1,2-hydrogen shift (e.g. HOOH → H₂OO) that must precede all of the oxygen transfers can be dramatically lowered by adding one or two molecules of solvent water. The solvent water forms a cyclic transition state and allows the hydrogen shift to occur by a 1,4 mechanism involving a proton relay. Likewise, one and two molecules of water are shown to decrease the barrier for NH₃ + H₂O₂ by ca. 20 kcal/mol per solvent water relative to isolated reactants or ca. 10 kcal/mol per water relative to solvated reactants. The same behavior is found for CH₃OOH. These data suggest that the accepted mechanism for oxygen atom transfer from the hydroperoxide functional group involving a direct displacement in concert with a 1,2-hydrogen shift must be modified to include the energetics of the 1,2-hydrogen shift. An ionic pathway for oxidation of NH₃ with H₂O₂ catalyzed by one water where the hydrogen is transferred after the rate-limiting oxygen transfer has a barrier 4.3 kcal/mol higher than the above concerted process.

Introduction

Few chemical transformations are as important and diverse as those involving oxygen atom transfer. The transfer of an oxygen atom involving cleavage of an oxygen–oxygen σ bond is one of the most significant biological transformations known,[1] and this type of oxidative insertion also enjoys a unique status in synthetic organic chemistry.[2] A detailed mechanistic picture of how such transformations occur remains the goal of both experimental and theoretical chemists. One of the problems that has impeded an understanding of the mechanism of oxygen atom transfer has been the long-standing perception historically that such oxidizing reagents are electrophilic in nature and hence the transferring oxygen has often been written as having a partial positive charge. The reacting partners, such as alkenes, amines and sulfides, in such oxidation reactions typically exhibit nucleophilic properties.

Consistent with this philosophy, when the nucleophilicity of a substrate such as a carbon–carbon double bond is enhanced by increasing alkyl substitution, the rate of oxygen atom transfer is increased. Conventional wisdom dictates that reagents of opposite charge have the highest attraction for each other. The idea of a highly reactive oxygen transfer reagent having a negatively charged "electrophilic" oxygen disturbs one's sensibilities, despite the fact that oxygen is the second most electronegative element.

(1) (a) Walsh, C. In *Flavins and Flavoproteins*; Vincent, M., Williams, C. H., Eds.; Elsevier/North Holland: Amsterdam, 1981; pp 121–132. (b) Walsh, C. In *Enzymatic Reaction Mechanisms*; W. H. Freeman and Co.: San Francisco, 1979; pp 406–463. (c) Bruice, T. C. In *Flavins and Flavoproteins*; Bray, R. C., Engel, P. C., Mayhew, S. E., Eds.; Walter DeGruyter and Co.: New York, 1984; pp 45–55.

(2) (a) Finn, M. G.; Sharpless, K. B. *Asymmetric Synth.* **1985**, *5*, 247. (b) Sheldon, R. A.; Kochi, J. *Metal-Catalyzed Oxidations of Organic Compounds*; Academic Press: New York; Chapter 9. (c) Mimoun, H.; Chaumette, P.; Mignard, M.; Saussine, L. *Nouv. J. Chim.* **1983**, *7*, 467.

[†] Wayne State University.
[‡] University of Manchester.

Table I. Optimized geometries and Energies for the 1,2–Hydrogen Shift of Hydrogen Peroxide

	HF/6-31G*	MP2/6-31G*	MP4SDTQ/6-31G*	HF/6-31G**	HF/6-311++G(2d,2p)
			HOOH (1)		
$R(O_1O_2)^a$	1.397	1.468	1.482	1.396	1.388
$R(O_1H_1)$	0.949	0.976	0.978	0.946	0.942
$\angle H_1O_1O_2{}^b$	102.07	98.65	98.61	102.31	102.97
$\angle H_1O_1O_2H_2$	115.36	121.02	120.95	115.44	111.22
E^c	−150.76479	−151.13492	−151.15080	−150.77696	−150.83215
$E_{MP4}{}^d$	−151.14614	−151.15074	−151.15080	−151.16989	−151.30477
$E_{ZPE}{}^e$	18.4	16.5			18.6
		HOOH →	H_2OO Transition State 1 (TS-1)		
$R(O_1O_2)^a$	1.602	1.576	1.633	1.601	1.588
$R(O_1H_1)$	1.190	1.426	1.425	1.184	1.187
$R(O_2H_1)$	1.094	1.035	1.038	1.081	1.083
$R(O_2H_2)$	0.951	0.980	0.980	0.947	0.943
$\angle H_1O_1O_2{}^b$	43.08	39.92	38.96	42.44	42.98
$\angle O_1O_2H_2$	100.49	98.57	96.89	101.01	101.53
$\angle H_1O_1O_2H_2$	106.04	104.06	104.22	106.77	105.33
E^c	−150.66641	−151.03923	−151.06247	−150.68271	−150.73517
$E_{MP4}{}^d$	−151.06658	−151.06148	−151.06247	−151.09382	−151.22639
$E_{ZPE}{}^e$	14.3	14.5			14.5
			H_2OO (2)		
$R(O_1O_2)^a$	1.606	1.517	1.563	1.606	1.570
$R(O_2H_1)$	0.951	0.979	0.980	0.946	0.944
$\angle H_1O_2O_1{}^b$	103.14	100.93	99.51	103.68	104.11
$\angle H_1O_2O_1H_2$	112.12	109.35	108.50	113.16	113.19
E^c	−150.70024	−151.05062	−151.07220	−150.71261	−150.76827
$E_{MP4}{}^d$	−151.06958	−151.07156	−151.07220	−151.09245	−151.23167
$E_{ZPE}{}^e$	17.5	16.9			17.7
$\Delta E_1^{\ddagger f}$	61.7	60.0		59.2	60.9
$\Delta E_2^{\ddagger}$	21.2	7.1		18.8	20.8
$\Delta E_1^{\ddagger}{}_{MP4}$	49.9	56.0	55.4	47.7	49.2
$\Delta E_2^{\ddagger}{}_{MP4}$	1.9	6.3	6.1	−0.9	3.3
$\Delta E_1^{\ddagger}{}_{ZPE}$	−4.1	−2.0			−4.1
$\Delta E_2^{\ddagger}{}_{ZPE}$	−3.2	−2.4			−3.2
$\Delta E_1^{\ddagger}{}_{MP4+ZPE}$	45.8	54.0	53.4	43.6	45.1
$\Delta E_2^{\ddagger}{}_{MP4+ZPE}$	−1.3	3.9	3.7	−4.0	0.1

a Bond lengths in Å. *b* Angles in deg. *c* Total energies in hartrees with geometry optimized at the level indicated. *d* MP2 energies are full, MP4 energies are frozen core. *e* Zero-point energies in kcal/mol. *f* Barriers in kcal/mol.

In previous studies we pointed out that the nucleophilic properties of an oxygen transfer reagent can serve to *increase* the rate of oxygen transfer.[3a] A great many electrophilic reagents have lone pairs of electrons on a heteroatom and their reactivity has far less to do with the charge on the atom than with the availability of a rapidly developing low-lying empty (electrophilic) orbital in the molecule that can accept a pair of electrons along the reaction coordinate. In a preliminary report of this work we have suggested that the idealized oxygen-transfer reagent should have an oxenoid oxygen with a full octet of electrons around the "electrophilic" oxygen.[4] In the present study we compare the "electrophilicity" of the oxygen atom in water oxide to that in ammonia oxide, a dipolar zwitterionic functional group that is familiar to most experimentalists.

Despite the generality of oxygen-transfer reactions, the literature is essentially void of high-level ab initio calculations involving oxygen transfer where an O–O bond is involved.[5] This is perhaps due in part to controversy surrounding the use of one of the simplest model oxidizing agents, hydrogen peroxide, that could

be used in high-level theoretical studies. Pople et al. reported[6a] that a 1,2-hydrogen shift in H_2O_2 to form water oxide (Table I) has a surprisingly high barrier ($\Delta E_1^{\ddagger}$ = 59.2 kcal/mol) with a transition structure that is 18.8 kcal/mol above the energy of water oxide at the HF/6-31G** level. However, at the MP4SDQ/6-31G**//HF/6-31G* level, with the E_{4T} triples contribution to the correlation energy calculated with the 6-31G* basis, the barrier for reversion of water oxide to H_2O_2 (ΔE_2^{*}) is eliminated entirely. It was concluded that water oxide cannot exist. In view of the fairly large basis sets involved, these facts have tended to discourage the use of H_2O_2 and related hydroperoxides as model compounds for theoretical studies.

The second and equally important enigma arose when we found that the activation barriers for oxygen transfer from H_2O_2 to nucleophiles such as ammonia or ethylene are actually higher than the barrier for the 1,2-hydrogen shift. For example, at the MP4SDTQ/6-31G*//HF/6-31G* level the barrier for the 1,2-hydrogen shift is 49.9 kcal/mol while the activation energy for concerted oxygen transfer from H_2O_2 to ammonia to form ammonia oxide is 52.1 kcal/mol.[7] At that same level the activation energy for the epoxidation of ethylene to form ethylene oxide is 67.5 kcal/mol. If it is assumed that oxygen atom transfer occurs from water oxide with little or no barrier, then the reaction surface

(3) (a) Bach, R. D.; Wolber, G. J. *J. Am. Chem. Soc.* **1984**, *106*, 1410. (b) Bach, R. D.; Coddens, B. A.; McDouall, J. J. W.; Schlegel, H. B.; Davis, F. A. *J. Org. Chem.* **1990**, *55*, 3325. (c) Bach, R. D.; McDouall, J. J. W.; Schlegel, H. B.; Wolber, G. L. *J. Org. Chem.* **1989**, *54*, 2931.

(4) Two preliminary reports on this work have appeared: Bach, R. D.; McDouall, J. J. W.; Owensby, A. L.; Schlegel, H. B. *J. Am. Chem. Soc.* **1990**, *112*, 7064, 7065.

(5) For a highly detailed theoretical study of the reaction of ozone with alkenes see: Cremer, D.; Bock, C. W. *J. Am. Chem. Soc.* **1986**, *108*, 3375 and references therein.

(6) (a) Pople, J. A.; Raghavachari, K.; Frisch, M. J.; Binkley, J. S.; Schleyer, P. v. R. *J. Am. Chem. Soc.* **1983**, *105*, 6389. (b) Schaefer, H. F., III *Acc. Chem. Res.* **1979**, *12*, 288.

(7) We are indebted to Prof. Ken Houk, who has related similar observations to us concerning hydrogen peroxide and peroxyformic acid.
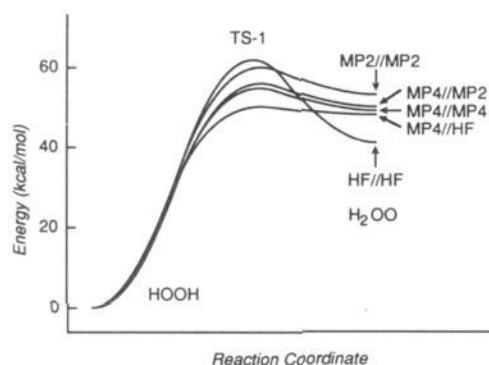
Figure 1. The role of electron correlation on the 1,2-hydrogen shift in the hydrogen peroxide → water oxide system (6-31G* basis set including ZPE at the level of theory indicated).

is dominated by the 1,2-hydrogen shift. Neither the significance of the barrier for this type of 1,2-hydrogen shift nor the fact that such reactions involved a two-step mechanism with an oxyoxonium ylide intermediate have been considered in the literature.

Results and Discussion

The Hydrogen Peroxide–Water Oxide Equilibrium. Our first task was to address the calculational difficulties encountered in the HOOH ⇌ H_2OO reaction. When the triples contribution to the MP4 energy barrier for the H_2O_2 rearrangement is calculated with the same basis set as the other contributions to the MP4 energy (i.e. 6-31G** which includes both d orbitals on heavy atoms and p orbitals on hydrogen) still no barrier was observed for the reverse reaction ($\Delta E_2^{\ddagger} = -0.9$ kcal/mol[4]). As noted in Table I, the potential energy surface for the 1,2-hydrogen shift remains almost unchanged at the Hartree–Fock level over a broad range of basis sets up to and including the 6-311++G(2d,2p) basis. With this highly polarized basis set the water oxide barrier ($\Delta E_2^{\ddagger}$) is 20.8 kcal/mol. However, with fourth-order Møller–Plesset correlation corrections applied to the HF geometries, $\Delta E_2^{\ddagger}$ is significantly reduced and zero-point energy corrections place the energy of water oxide nearly equal to or above the energy of the transition structure for all three cases where the geometry was optimized at the Hartree–Fock level.

Because of the computational expense involved, typical protocol is to calculate the correlation correction with use of a Hartree–Fock optimized geometry. The marked effect of correlation correction on the relative energy of water oxide suggested that Hartree–Fock theory gave a poor representation of both the O–O single bonds and the zwitterionic structure. When the 1,2-hydrogen shift of H_2O_2 was optimized at the MP2/6-31G* level we found a radically different energy profile (Figure 1). The MP4SDTQ/6-31G*//MP2/6-31G* barrier for the hydrogen shift is 56.0 kcal/mol. Significantly, water oxide exists as a local minimum 6.3 kcal/mol lower in energy than the transition structure, although with ΔZPE this barrier is reduced to 3.9 kcal/mol. Thus, water oxide does exist and could potentially serve as a donor of singlet oxygen atoms. At the MP2 level the O–O bond distance in H_2O_2 is now in agreement with experiment (1.468 vs 1.475 Å)[6] and the O–O bond in water oxide is considerably shortened (0.09 Å) while the O_1–H_1 bond in TS-1 is lengthened (0.24 Å) by the MP2 correlation correction. Optimization at the MP4/6-31G* level did not result in a meaningful improvement over the MP2 potential energy surface, and we have concluded that the MP2 level of theory adequately describes the O–O bond lengths.

Orbital Interactions Involving 1,2-Hydrogen Shifts in H_2O_2 and NH_2OH. The species derived from a simple 1,2-hydrogen shift from a singly bonded normal valence structure to an adjacent lone pair of electrons can be formally represented as complexes of singlet oxygen atom with Lewis bases such as H_2O and NH_3. Such transformations involving formation of H_2OO and NH_3O by a 1,2-hydrogen shift in H_2O_2 or NH_2OH typically have relatively high barriers for the forward reaction to form a dipolar molecule
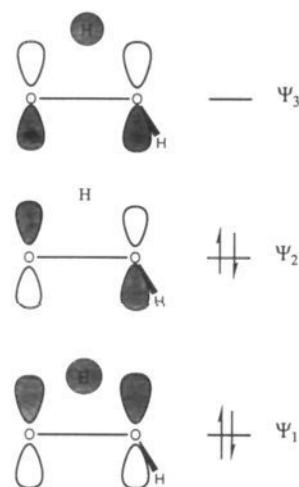

Figure 2. Frontier molecular orbitals for the three-MO four-electron interaction involving a 1,2-hydrogen shift in hydrogen peroxide.

and comparatively small barriers for the reverse reaction, affording the normal covalent structure. A clear exception to this generality is ammonia oxide. The origin of the high barriers (ca. 50 kcal/mol)[6] for 1,2-hydrogen shifts in such reactions as HOF → HFO, H_2NNH_2 → H_3NNH, and the H_2O_2 and NH_2OH rearrangements described herein lies partially in the fact that these are four-electron systems. For example, Wagner–Meerwein rearrangement involving 1,2-hydrogen shifts to an adjacent empty 2p orbital on carbon is a two-electron three-center process that typically has an activation barrier less than 5 kcal/mol. In contrast, H_2O_2 has an abundance of lone pairs of electrons and consequently the migration surface involves filled orbitals with π^*-type symmetry. In principle, such 1,2-rearrangements involving four electrons have been labeled as formally forbidden. However, 1,2 shifts of this type necessarily involve mixing of the adjacent lone pair on the heteroatom with both the σ and σ^* orbitals of the O–H bond. In this three-MO four-electron process the lowest bonding MO (Ψ_1) will be bonding throughout the hydrogen migration across the O–O bond (Figure 2). In the HOMO (Ψ_2) where the doubly occupied in-plane p orbitals are of opposite phase, the migrating hydrogen must undergo a phase change in order to break the initial O–H bond and effect bonding at the migration terminus. Consequently, orbital symmetry considerations require that the migrating hydrogen be nonbonding in HOMO (Ψ_2) at or near the transition state for the 1,2 migration. Thus, the reaction is not forbidden, but as a result of orbital phase cancellation[3] it has an occupied nonbonding orbital that contributes to the high barrier. This same logic possibly provides an explanation for why 1,2-hydrogen migration in the well-studied prototype singlet vinylidene–acetylene isomerization, H_2CC → HCCH, has a low barrier (5–8 kcal/mol) while the hydroxy-carbene–formaldehyde rearrangement exhibits a sizable barrier of ~35 kcal/mol.[6b] In the former case, the hydrogen can migrate to an empty p orbital on the carbenoid carbon while in the latter the adjacent lone pair of electrons on oxygen will require 1,2-hydrogen migration to a filled orbital if the transition state has appreciable carbon–oxygen double bond character.

We felt that it would be instructive to test the validity of these conclusions by examining a structurally related compound that exhibits different chemistry. For example, hydroxylamine, which contains one less unshared pair of electrons, has a 1,2-hydrogen shift barrier (55.9 kcal/mol) virtually identical with that of hydrogen peroxide, but in this case the resulting dipolar ammonia oxide is much more stable in the gas phase.[6a] The relatively high barrier for the reverse 1,2-hydrogen shift to form ground-state hydroxylamine is atypical for this class of compounds. Hydroxylamine is not an effective oxygen donor, but tertiary amine oxides are mild oxidizing agents. A comparison of the two oxygen donors at the same level of theory demonstrates that the theoretical data are in good accord with experiment.

Table II. MP2/6-31G* and HF/6-31G* (in parentheses) Geometries and Energies for Hydroxylamine → Ammonia Oxide[a]

$$H_1 \overset{\Delta E_3^{\ddagger}}{\rightleftharpoons} \quad \overset{\Delta E_4^{\ddagger}}{\rightleftharpoons}$$

(structures: 3, TS-2, 4)

|	H₂NOH (3)	transition state 2	H₃NO (4)[d]
$R(NO)$	1.451 (1.403)	1.507 (1.513)	1.362 (1.376)
$R(OH_1)$	0.971 (0.946)	1.350 (1.239)	
$R(NH_2)$	1.021 (1.002)	1.017 (0.997)	1.036 (1.010)
$\angle H_1ON$[b]	101.32 (104.19)	44.53 (45.90)	
$\angle H_2NO$	102.91 (104.76)	110.52 (109.31)	113.17 (111.70)
$\angle H_1ONH_2$	125.34 (124.03)	116.55 (116.94)	
$E_{MP2(HF)}$	−131.330 17 (−130.978 84)	−131.240 36 (−130.874 43)	−131.283 13 (−130.933 89)
E_{MP4}[b]	−131.349 57 (−131.346 53)	−131.260 46 (−131.260 08)	−131.302 67 (−131.300 97)
$\Delta E_3^{\ddagger}{}_{MP2(HF)}$[c]		56.4[e] (65.5)[f]	
$\Delta E_4^{\ddagger}{}_{MP2(HF)}$		26.8[e] (37.3)[f]	
$\Delta E_3^{\ddagger}{}_{MP4}$		55.9[g] (54.2)[h]	
$\Delta E_4^{\ddagger}{}_{MP4}$		26.5[g] (25.7)[h]	

[a] Bond lengths in Å, angles in deg, total energies in hartrees. [b] Energy refers to MP4(SDTQ) with frozen core approximation. [c] Barriers in kcal/mol without zero-point energy (ZPE). [d] C_{3v} symmetry. [e] MP2/6-31G*//MP2/6-31G*. [f] HF/6-31G*//HF/6-31G*. [g] MP4/6-31G*//MP2/6-31G*. [h] MP4/6-31G*//HF/6-31G*.
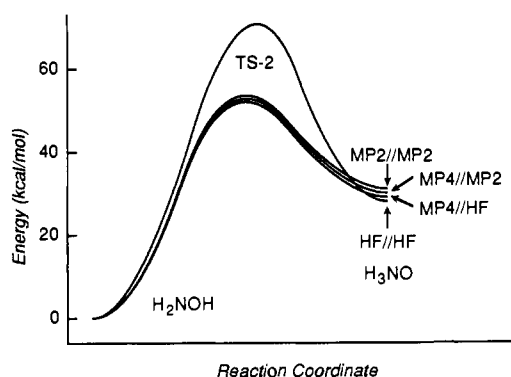

Figure 3. The role of electron correlation on the 1,2-hydrogen shift in the hydroxylamine → ammonia oxide system (6-31G* basis set without ZPE at the level of theory indicated).

Calculation of the energy at the MP4SDTQ level with the HF/6-31G* geometries[8] lowered both the forward and the reverse hydrogen shift barriers in the NH₂OH system by about 11 kcal/mol (Table II) in marked contrast to the hydrogen peroxide system where the effect of electron correlation for water oxide is much more pronounced. The second major difference between these two processes is that optimization at the MP2/6-31G* level had no significant effect on either barrier (calculated at the MP2 or MP4 levels), and the depths of the potential energy well (26.8 kcal/mol) for ammonia oxide was not significantly altered (Figure 3).

Oxygen Transfer from Hydrogen Peroxide to Ammonia. The generally accepted mechanism[1] for oxygen transfer from an alkyl hydrogen peroxide is attack by the substrate on the distal oxygen with a direct nucleophilic displacement of the β-peroxy oxygen. Hydrogen migration is assumed to occur simultaneously (eq 1).

$$R-O \cdots X \longrightarrow R-O + O-X \tag{1}$$

$$X: = N:, -S^-, I^-$$
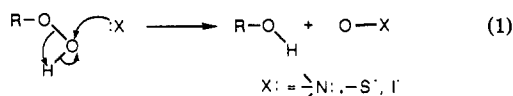
(8) (a) Molecular orbital calculations have been carried out with the GAUSSIAN 88 progran system[8b] utilizing gradient geometry optimization.[8c] (b) Frisch, M. J.; Head-Gordon, M.; Schlegel, H. B.; Raghavachari, K.; Binkley, J. S.; Gonzalez, C.; DeFrees, D. J.; Fox, D. J.; Whiteside, R. A.; Seeger, R.; Melius, C. F.; Baker, J.; Martin, R. L.; Kahn, R. L.; Stewart, J. J. P.; Fluder, E. M.; Topiol, S.; Pople, J. A. Gaussian, Inc., Pittsburgh, PA, 1988. (c) Schlegel, H. B. *J. Comp. Chem.* **1982**, *3*, 214. (d) Gonzalez, C.; Schlegel, H. B. *J. Chem. Phys.* **1989**, *90*, 2154. (e) Eade, R. H. A.; Robb, M. A. *Chem. Phys. Lett.* **1981**, *83*, 362. (f) Pople, J. A.; Head-Gordon, M.; Raghavachari, K. *J. Chem. Phys.* **1987**, *87*, 5968.
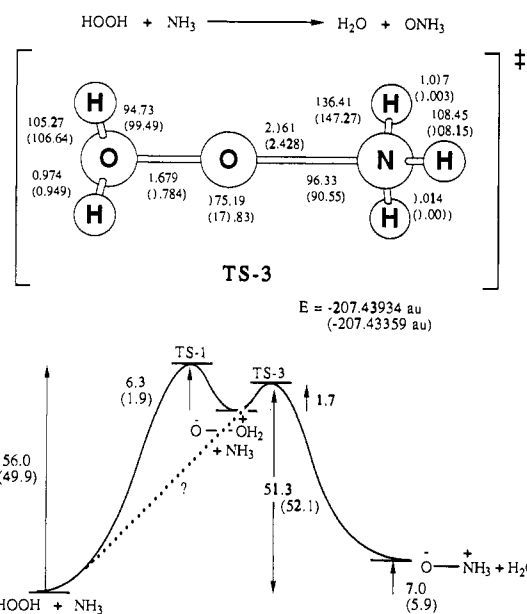
Figure 4. (a, top) Optimized transition structure at the MP2/6-31G* level (HF/6-31G* geometry in parentheses). (b, bottom) A comparison of the potential energy surfaces for 1,2-hydrogen shift (kcal/mol) in and oxygen atom transfer from hydrogen peroxide at the MP4SDTQ/6-31G* level (no ZPE) with use of the MP2 optimized geometry (MP4 energies at the HF geometries in parentheses).

The concerted transfer of an oxygen atom from H₂O₂ to NH₃ involves both a 1,2-hydrogen shift and the simultaneous transfer of the oxygen by an SN2-like cleavage of the O–O bond. We were able to locate a stationary point on the reaction surface where the hydrogen had not completely migrated, but this structure was a third-order saddle point. The transition structure, which is a first-order saddle point as established by a frequency calculation at the HF level, has the hydrogen completely shifted and closely resembles water oxide and ammonia. In fact, the barrier calculated (MP4SDTQ/6-31G*//MP2/6-31G*) from ground-state water oxide plus ammonia is only 1.7 kcal/mol. That same transition structure (TS-3) may potentially arise from an SN2 displacement by H₂O on H₃NO, but this barrier, because of ground-state-energy differences, is 44.3 kcal/mol above reactants (Table III). The optimized geometry of the transition structure and the potential energy profile are shown in Figure 4. It is gratifying that at the MP4/6-31G*//MP2/6-31G* level of theory the oxygen-transfer barrier is now 4.7 kcal/mol lower than the 1,2-hydrogen shift transition state. However, when the reaction

Table III. Total Energies and Activation Barriers for Intermediates and Transition States for Oxygen Atom Transfer

	HF/6-31G*	MP4//HF/6-31G*	ΔEMP4//HF	MP2/6-31G*	MP4//MP2/6-31G*	ΔEMP4//MP2
TS-3	-206.88272	-207.43359	52.1	-207.40066	-207.43934	51.3
TS-4	-187.06981	-187.61739	62.5	-187.58100	-187.62293	59.0
TS-5	-226.70832	-227.26578	54.4	-227.23913	-227.27445	52.5
TS-6a	-189.64561	-190.19271	81.2	-190.15929	-190.19434	83.4
TS-6b	-189.69767	-190.24362	49.3	-190.20669	-190.24004	54.7
TS-6c	-245.91031	-246.60728	53.5			
TS-6d	-321.94014	-322.84433	34.3			
TS-7	-226.69415	-227.29696	34.8			
TS-8		-227.30647	28.9			
TS-9	-282.91404	-283.67228	31.8	-283.63642	-283.68168	29.4
TS-9a	-282.86778					
TS-9b				-283.63562	-283.67478	33.7
TS-10	-358.94113	-359.90550	14.9	-359.86525	-359.91795	11.2
TS-11	-302.73614	-303.54001	11.8	-303.51787	-303.54650	11.9
TS-12	-207.23963	-207.83093	-29.4			
5	-189.79670	-190.32210		-190.29944	-190.32724	
6	-189.73233	-190.24932		-190.21902	-190.25126	
7	-226.78685	-227.36730		-227.35034	-227.37359	
8	-226.73247	-227.30870		-227.28752	-227.31386	
9	-302.81115	-303.59635		-303.56985	-303.60029	
10	-302.76556	-303.54723		-303.52253	-303.55429	
12	-151.03296	-151.41363				

path is followed back from the transition state,[8d] it leads toward water oxide plus ammonia and not to H_2O_2 + NH_3, which strongly suggests that this is a two-step process. The most significant geometry changes are in the N–O bond in H_3NO and the O–O bond in H_2OO of the transition structure where the bonds calculated at the MP2 level are shorter than those calculated at the Hartree–Fock level by as much as 0.27 Å. Frequency calculations at the MP2 level (using CADPAC) confirm that this structure has an appropriate transition vector. A second imaginary frequency (110i cm^{-1}) corresponds to a rotation of the NH_3 group about the N–O axis; optimization leads to a 0.03 kcal/mol lower transition state. The overall reaction is slightly endothermic (7.0 kcal/mol) despite the fact that the N–O bond is considerably stronger than the O–O bond. The estimated bond dissociation energy of the O–O bond in water oxide is only 4.6 kcal/mol lower than that in hydrogen peroxide.[9a]

The necessity for optimization at the MP2 level appears to be general for reactions involving H_2O_2 since the MP4SDTQ/6-31G* barrier for concerted oxygen transfer from H_2O_2 to ethylene has been lowered from 67.5 to 50.1 kcal/mol with MP2 optimization. Water oxide continues to be the most effective oxene donor that we have identified since the barrier affording ethylene oxide from ground state water oxide at this MP2 level is only 0.4 kcal/mol. We may conclude that the overall difficulty with oxygen transfer from hydrogen peroxide is definitely not a basis set problem but rather one of the necessity for electron correlation to adequately describe the dipolar O–O bond in water oxide. A concerted gas-phase oxygen atom transfer from H_2O_2, in the absence of bath gas participation, would be highly unlikely in view of the magnitude of the barriers involved.

Because of the inherent difficulty in treating O–O bonds rich in lone pairs, as well as elongated bonds in the TS,[10] the question of SCF stability should be examined for H_2OO + NH_3 → H_2O

+ O–NH_3 and related transition states with 1 and 2 molecules of solvent water (see below). When 0, 1, and 2 water molecules are involved in the TS the MP2/6-31G* O–O bond distances are 1.68, 1.70, and 1.72 Å and the roots of the RHF → UHF stability analysis vary from -0.03, -0.01 to +0.01. As the number of water molecules increase the N–O bond distances in the TS decrease by 0.18 Å. The TS (see TS-10) with the longer O–O (1.722 Å) and shorter N–O bond (1.978 Å) is RHF stable which suggests that hydrogen bonding plays a role in stabilizing the transition structure and in making it more product-like. Release of the RHF constraints (HF/6-31G*) and reoptimization of the molecular orbitals in TS-3 (MP2/6-31G* geometry) affording a UHF stable wave function resulted in a decrease in total energy of only 1.8 kcal/mol. The stability analysis indicates that the p-type lone pairs on the central oxygen of TS-3 want to mix with several of the lowest unoccupied orbitals.

To assess the importance of this orbital mixing we performed CASSCF calculations and reoptimized geometries using the 6-31G* basis.[8e] In considering the geometry of the transition state it is useful to divide the system into three components: NH_3 + O + H_2O. For the choice of active space (i.e. orbitals that are allowed to possess variable occupancy) we need only consider the valence shells of atoms other than hydrogen. In NH_3, the nitrogen atom is in an sp^3 state with five electrons; since three unpaired electrons go to form the inactive N–H bonds, the remaining orbital with a lone pair of electrons must be included in the active space. In the central oxygen atom, the valence shell consists of two singly occupied p orbitals, which contribute to the partially broken O–O bond and the partially formed N–O bond, and two lone pairs in 2s and 2p orbitals, respectively. All six electrons and four orbitals must be included in the active space. Finally in the H_2O moiety, two unpaired electrons form the sp^3 oxygen go to form the O–H bonds and can be ignored, leaving the two lone pair orbitals to be included in the active space. In total this yields 12 electrons in 7 orbitals (28 configurations) and includes all valence shell orbitals and electrons that are not involved in bonding to hydrogen. Re-optimization of the transition-state geometry at this internally correlated level reduces the N–O bond from 2.428 Å (HF/6-31G*) to 2.302 Å and increases the O–O bond from 1.784 (HF/6-31G*) to 1.833 Å. The CASSCF natural orbitals yield an occupancy for the LUMO of 0.051 electron, indicating some contribution from excited configurations but only a rather small degree of electron transfer. The excitation into the LUMO arises from an almost equal contribution from the two lone pairs on the central oxygen atom and the lone pair directed along the O–O bond in the H_2O moiety. The lone pair on nitrogen, directed along the N–O bond, remains doubly occupied. From this we conclude that the effect of electron transfer is negligible in this structure.

(9) (a) The BDE (kcal/mol) of the O–O (44.6) and N–O (87.3) bond was estimated by calculating (MP4SDTQ/6-31G*//MP2/6-31G*) the dissociation of H_2O–O and H_3N–O into a singlet (^1D) oxygen atom and H_2O or NH_3. The O–O bond in H_2O_2, relative to two hydroxyl radicals, is 49.2 kcal/mol, in good agreement with experiment (51 kcal/mol).[9b] The O–O BDE is only 0.14 kcal/mol at HF/6-31G*, reflecting the importance of the electron correlation correction. (b) Cremer, D. The Chemistry of Functional Groups. In *Peroxides*; Patai, S., Ed.; John Wiley & Sons: New York, 1983; p 1.

(10) At the MP2 geometry, stability tests show that the SCF wave function for HOOH and H_2OO are stable while TS-1 is real RHF to real UHF unstable but with a very small negative root of -0.0069. At the HF geometry water oxide is also unstable with a root of -0.03. The addition of two water molecules affords a transition structure (TS-10) that is real RHF to real UHF stable. Because of problems caused by spin contamination, MP4 calculations based on the RHF wave function are more reliable than those based on a UHF wave function.
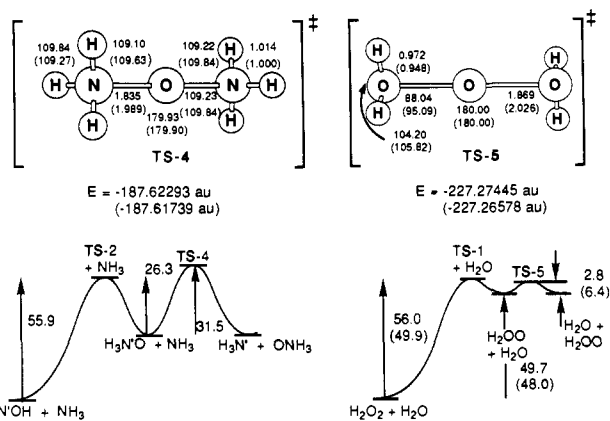
Table IV. Effect of Electron Correlation of the Bond Distances (Å) for Oxygen Atom Transfer to Ammonia in TS-3 (6-31G*, Basis)

level of calculation	O–O	N–O
HF	1.784	2.428
CASSCF	1.833	2.302
CISD	1.719	2.234
QCISD	1.721	2.278
MP2	1.679	2.161

This is a significant result because nucleophilic attack at an electron-rich center, with the potential for a rapidly developing low-lying (electrophilic) empty σ^*_{O-O} orbital upon elongation of the relatively weak O–O bond, would appear to present an ideal opportunity for electron transfer. We are particularly intrigued by the total absence of electron transfer from the lone pair on the nucleophilic nitrogen to the σ^*_{O-O} orbital as one might anticipate for this type of S_N2 process.

As a further test of the sensitivity of the transition state to correlation corrections, calculations were carried out at two additional levels of theory: CISD, configuration interaction with all single and double excitations, and QCISD, quadratic configuration interaction[8f] (which is size consistent and includes the effect of quadruple excitations). Experience with a large set of two-heavy-atom molecules containing lone pairs suggests that bond distances calculated at second-order Moller–Plesset (MP2/6-31G*) tend to be a little larger than experimental values, while Hartree–Fock bond distances are too short. Bond length deficiencies in equilibrium structures are largely removed at the MP3/6-31G* and CID/6-31G* levels,[11] and the CISD and QCISD levels should be even better. In particular, QCI calculations do very well in reproducing the energies of highly distorted systems that can display substantial configurational mixing,[8f] and hence should be well-suited for transition structures. As can be seen from the summary in Table IV, the CISD and QCI bond lengths in the transition state are very similar; both are substantially shorter than the Hartree–Fock values but somewhat longer than the MP2 bond lengths. The CISD and QCISD barriers (3.0 and 2.2 kcal/mol, respectively) are both slightly lower than the MP2 barrier (4.6 kcal/mol). The QCISD results can be compared directly with the MP4SDQ data (neither includes triple excitations); the QCI values agree very well with the MP4SDQ barriers at either the MP2 or the QCISD optimized geometry (2.9 and 3.0 kcal/mol, respectively). As noted above the barrier calculated with MP4SDTQ level (i.e. including triple excitations) at the MP2 geometry is 1.66 kcal/mol. Thus, all correlated levels of theory consistently afford an exceptionally low barrier for oxygen atom transfer from water oxide to ammonia. Furthermore, from the comparison of the MP4SDQ barriers calculated at the MP2 and QCISD geometries, it is apparent that MP2 optimization is sufficient to describe the geometry of these unusual transition states.

A Comparison between Water Oxide and Ammonia Oxide. Mechanistic insight relating to oxygen atom transfer may also be gained by studying model identity reactions involving NH_2OH + NH_3 and H_2O_2 + H_2O. The activation barrier for the identity reaction of oxene transfer from ammonia oxide to ammonia (Figure 5a) is 31.5 kcal/mol versus the 1.7 kcal/mol calculated for water oxide at the same level. Significantly, this barrier is 5 kcal/mol higher than that for reversion of ammonia oxide to NH_2OH. The overall barrier for a concerted process involving a 1,2-hydrogen shift accompanying the S_N2 displacement on NH_2OH would be 60.9 kcal/mol. Since this transition structure is a first-order saddle point, by analogy to the oxygen transfer from H_2O_2 to NH_3, the transition states for concerted and two-step processes are very likely identical. A recent study by Bachrach[12a]

(11) DeFrees, D. J.; Raghavachari, K.; Schlegel, H. B.; Pople, J. A. *J. Am. Chem. Soc.* **1982**, *104*, 5576.

(12) (a) Bachrach, S. M. *J. Org. Chem.* **1990**, *55*, 1016. (b) Beak, P.; Allen, D. J.; Lee, W. K. *J. Am. Chem. Soc.* **1990**, *112*, 1629. (c) The calculated charge on oxygen with use of Baders' Topological Density Analysis is more typically −1.2 to −1.3. For a discussion see: Bachrach, S. M.; Streitwieser, A. *J. Comput. Chem.* **1989**, *10*, 514.

Figure 5. (a, left) 1,2-hydrogen shift (**TS-2**) versus oxygen atom transfer (**TS-4**) in hydroxylamine, (b, right) 1,2-hydrogen shift (**TS-1**) versus oxygen atom transfer (**TS-5**) in hydrogen peroxide (optimized transition structures at the MP2/6-31G* level, HF/6-31G* geometry in parentheses; MP4SDTQ/6-31G*//MP2/6-31G* relative energies in kcal/mol (no ZPE), MP4SDTQ/6-31G*//HF/6-31G* values in parentheses).

established that the identity displacement reaction, H_3NO + NH_3 → H_3N + ONH_3, proceeded without an intermediate and had a barrier of 37.3 kcal/mol at the MP2/6-31G* level. The N–O–N bond angle in the TS is essentially linear and deviation from a 180° approach for this S_N2 attack at the nonsterogenic oxygen atom results in a relatively steep increase in energy. For example, calculated relative energies (HF/6-31G*) for transition structure geometries with N–O–N bond angles of 180°, 170°, 160°, and 150° are 0, 0.9, 3.5, and 7.5 kcal/mol, respectively. Experimental data describing an endocyclic restriction test for a near linear S_N2 transition structure have recently appeared.[12b] From these data it may be concluded that both H_2O_2 and NH_2OH must undergo a 1,2-hydrogen shift prior to reaction with a nucleophile. The reaction pathway for NH_2OH may also be thwarted by an unfavorable equilibrium for the 1,2 shift that lies on the side of the starting material. Both oxygen-transfer reactions exhibit very high gas-phase barriers and hence their reactions in aqueous solution must be highly solvent dependent. Hydroxylamine should hydrogen bond more strongly than hydrogen peroxide since their respective proton affinities (HF/6-31G*) are 211.3 and 168.2 kcal/mol. Secondary amine oxides rapidly rearrange to hydroxylamines in aqueous solutions and consequently the formation of NH_2OH ($\Delta E_3^‡$) must be catalyzed by water in a protonation–deprotonation sequence. Studies that include waters of solvation for oxygen transfer from water oxide are given below.
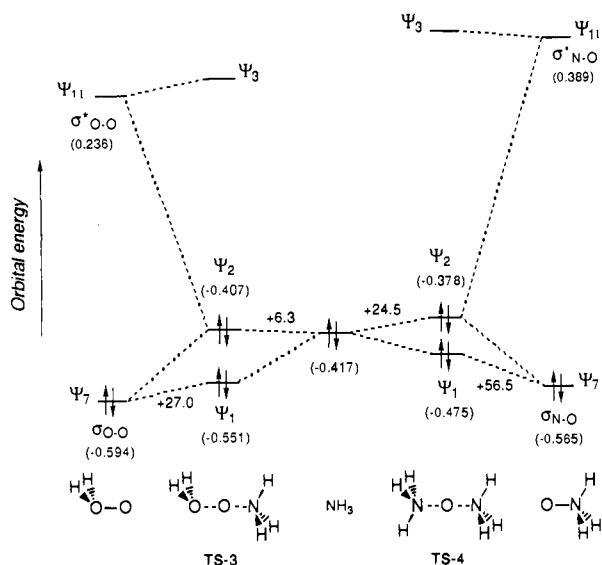
The comparable identity reaction involving S_N2 displacement by a water molecule on water oxide (Figure 5b) has an activation barrier of only 2.8 kcal/mol. That activation energy is of course much higher (24.4 kcal/mol) if calculated from water oxide hydrogen bonded to a water molecule (8, Figure 10) instead of isolated reactants. These data suggest that an equilibrium involving oxygen atom transfer between water oxide and water (**TS-5**) would be energetically feasible. It should be noted that both transition states involving oxygen atom transfer from H_2OO to either NH_3 (**TS-3**) or H_2O are comparable in structure with relatively long O–O bonds.

The remarkable difference in reactivity between water oxide and ammonia oxide toward nucleophilic displacement merits additional comment. Both oxygen-transfer reagents have the requisite full octet of electrons around their "electrophilic" oxygens and they afford a neutral leaving group after oxygen atom transfer. One indication of the origin of the relative propensity for oxene donation for these two reagents comes from an examination of the changes in orbital energies on going from the ground to the transition state for the S_N2 displacement reactions with ammonia (Figure 6).

The energy levels of the two σ bonds being broken do not differ significantly, but the N–O σ^* orbital is appreciably higher in energy (0.153 au) than the O–O σ^* orbital in water oxide. The

Figure 6. Three-MO, four-electron interactions providing a comparison of the HF/6-31G* molecular orbital energies (Ψ_1, Ψ_2, and Ψ_3) for oxygen atom transfer (a, left) from water oxide to ammonia (**TS-3**) and (b, right) ammonia oxide to ammonia (**TS-4**) (orbital energies in au; energy differences in kcal/mol).

three-MO four-electron interaction[3] of the HOMO of NH_3 with the bonding and antibonding orbitals of the σ bond increases the energy of Ψ_1 and Ψ_2 in both the H_2OO-NH_3 and H_3NO-NH_3 transition states. In **TS-3** the HOMO of :NH_3 is not extensively mixed into the σ^* orbital of water oxide and its energy level is increased by only 6.3 kcal/mol as a consequence of its four-electron interaction with the filled σ O–O orbital. Consistent with these data, the H_3N---O bond is fairly long at 2.16 Å and the O–O bond in **TS-3** has only been elongated by 11%. In symmetrical **TS-4** both N–O bonds have been stretched by 35%, and these orbital interactions are reflected in a 24.5 kcal/mol energy increase in the HOMO level of the nucleophile ammonia. The basic tenets of FMO theory suggest that upon orbital mixing the bonding combination will be stabilized and the complementary out-of-phase orbital will be increased in energy. However, extensive bond deformation of one of the reactants in the transition structure can result in a significant energy increase[3c] in all frontier MOs of the TS. The difference in activation barriers of 28.7 kcal/mol for these two oxygen transfer reactions is clearly reflected in the fact that the combined increase in energy of Ψ_1 and Ψ_2 (Figure 6) is 33.3 kcal/mol in **TS-3** and 81.0 kcal/mol in **TS-4**.

The increase in energy of H_2O_2 and NH_2OH upon undergoing hydrogen transfer is also partly reflected in the destabilization of their resulting dipolar bonds. For example, the energy level of these σ bonds increases by 82.8 and 71.5 kcal/mol, respectively, upon conversion to H_2OO and H_3NO. This obviously makes the HOMO levels closer in energy and increases the four-electron splitting which facilitates the oxygen-transfer reaction by enhancing the interaction of the developing HOMO in the transition state with the empty σ^* orbital of the O–O bond. This perturbation is attended by a decrease in the energy level of the σ^* orbital and hence an increase in its electrophilicity as the O–O bond is elongated along the reaction pathway.[3a] From an enthalpic point of view the O–O and N–O bond dissociation energies (BDE) of water oxide and ammonia oxide have been estimated to be 45 and 87 kcal/mol, respectively.[9a] Thus, a combination of electron repulsion between the lone pair on ammonia with that on oxygen in the transition state and the stronger N–O bond appear to be largely responsible for its low reactivity as an oxygen donor. The reluctance of H_3NO to transfer its oxygen atom is also reflected in a relatively high barrier for alkene epoxidation. While the activation energy (MP4SDTQ/6-31G*//HF/6-31G*) for oxygen transfer from H_3NO to NH_3 is 33.9 kcal/mol, the corresponding reaction with ethylene to form ethylene oxide has a barrier of 27.6 kcal/mol. In contrast, oxygen transfer from water oxide to
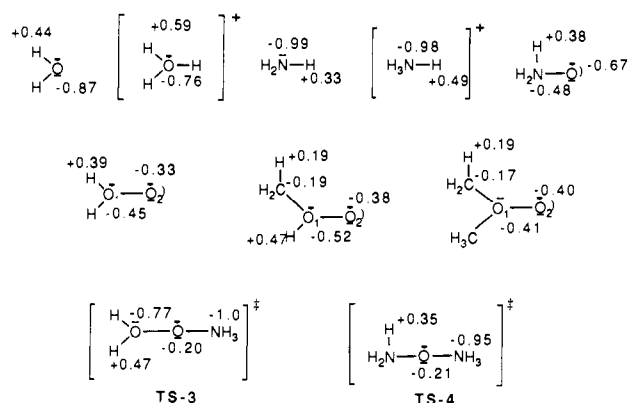

Figure 7. A comparison of formal charges with calculated Mulliken charges (HF/6-31G*).

ethylene at this level occurs with a barrier of 19.4 kcal/mol. The latter reaction provides yet another example of the role of MP2 geometry optimization since this barrier is reduced to 0.4 kcal/mol at the MP4SDTQ/6-31G*//MP2/6-31G* level of theory. The fact that the oxygen on an N-oxide bears a formal negative charge is merely coincidental because water oxide is also zwitterionic, has a full octet of electrons around the transferring oxygen, and yet is one of the most reactive oxidants that we have yet encountered.

Since the experimentalist has historically preferred to consider electrophilic species with at least a partial positive charge on the electrophilic atoms, perhaps a discussion of how the atom charges change on going from ground state to transition state would be useful. First, it should be pointed out that the use of the classical formal charge can be misleading. For example, the formal charges on oxygen and nitrogen in the hydronium and ammonium ions are +1. However, the calculated Mulliken charges are –0.76 and –0.98, respectively.[12c] Similarly, the formal charge on O_1 in water oxide is +1 while its calculated charge of –0.45 is actually higher than that on O_2 (Figure 7). However, the atomic charge on O_1 is +0.33 when the H_2O fragment of water oxide has the positive charges on hydrogen summed into those of the heavy atoms. A similar treatment of methanol oxide affords a net charge on O_1 of –0.03 while the charge on O_1 in dimethyl ether oxide remains at –0.41. In both transition states the NH_3 fragment acquires very little additional charge while the charge on the central oxygen O_2 is diminished. Since the electrophilicities of water oxide and methanol oxide are quite comparable it is obvious that neither the formal nor the calculated charges should be used as a guide to reactivity. Both reagents may be formally considered to be an oxene atom bound to water or methanol (oxenoid). As advocated previously,[3] the electrophilic nature of such species may be attributed to how readily an empty σ^* orbital is lowered in energy as its σ bond is stretched along the reaction coordinate. Since the O–O σ bond is relatively weak and the oxenoid nature of the transferring oxygen is initially repulsive in nature and induces O–O bond elongation upon interaction with a nucleophile, such species exhibit excellent electrophilic behavior.

The above comparison of activation barriers concentrated mainly on the difference between the transition states for oxygen atom transfer. The overall gas-phase potential energy surface for oxidation of ammonia by H_2O_2 is given in Figure 8. Although the ground state of the donor has an oxenoid oxygen, the transferring oxygen in the transition structures for many of these reactions resembles a singlet oxygen atom (oxene). The minimum energy structure that is a complex between H_2O_2 and NH_3 is stabilized by 11.4 kcal/mol (MP4SDTQ/6-31G*//MP2/6-31G*) while on the products side the hydrogen-bonded complex between ammonia oxide and water exists at a minimum of 19 kcal/mol below the isolated products. Significantly, water oxide is stabilized by ammonia in a cyclic array by 22.6 kcal/mol (cf. Figure 4) which is indicative of an exceptionally strong hydrogen bond at the oxenoid oxygen. The barrier for the oxygen-transfer step from this water oxide complex is 24.3 kcal/mol. In the absence of
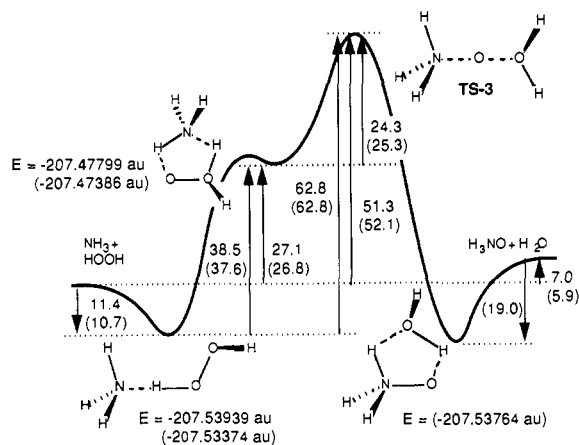
Figure 8. The potential energy profile for oxygen atom transfer from H_2O_2 to NH_3 at the MP4SDTQ/6-31G*//MP2/6-31G* level in kcal/mol; MP4 energies with use of the HF optimized geometries in parentheses.

solvent, the barrier for oxygen transfer from H_2O_2 is obviously dominated by the energetic requirements for the 1,2-hydrogen shift. A similar situation was noted for the direct S_N2 displacement of ethylene on H_2O_2 affording protonated ethylene oxide and hydroxide ion. In the absence of solvent assistance, the products for this ionic gas-phase process lie 194.0 kcal/mol (MP2/6-31G*) above reactants ethylene and hydrogen peroxide and a prohibitively high barrier should be anticipated. The O–O bond distance in a transition state for oxygen transfer from H_2O_2 is typically longer than that in the TS for a hydrogen shift in H_2O_2. Since the barrier for the 1,2-hydrogen shift is increased markedly when the O–O bond is lengthened (e.g. from 1.6 to 2.0 Å the barrier increases from 61.7 to 83.5 kcal/mol), the hydrogen should be transferred either prior to or after oxygen atom transfer in the absence of solvent or ROOH participation.

Oxygen Atom Transfer from ROOH. We also tested the generalities of these conclusions by examining the comparable potential energy surface for an alkyl hydrogen peroxide. As anticipated the MP4SDTQ/6-31G*//HF/6-31G* barrier (49.3 kcal/mol) for the 1,2-hydrogen migration of methyl hydrogen peroxide (5) to afford methanol oxide (6, Figure 9a) is virtually identical with that of hydrogen peroxide. A small barrier for the reverse process, $\Delta E_{6b}^* = 3.6$ kcal/mol, is also in evidence in the absence of zero-point correction. It was therefore essential to calculate these barriers with optimization at the MP2 level to establish the intermediacy of methanol oxide (6). At the MP4SDTQ/6-31G*//MP2/6-31G* level $\Delta E_{5b}^* = 54.7$ kcal/mol and $\Delta E_{6b}^* = 7.0$ kcal/mol, which suggests that methanol oxide is a stable though transient gas-phase species. Thus, the barrier for oxygen atom transfer from an alkyl hydrogen peroxide should also be largely comprised of the energy requirements for the 1,2-hydrogen migration. Since methanol oxide can also be formed by a 1,2-methyl shift (**TS-6a**) we calculated that activation energy and as anticipated it was much higher (83.4 kcal/mol) than the hydrogen shift barrier. In the latter pathway the possibility for a 1,4-proton shift involving water catalysis is also possible but will most likely also have a high barrier by analogy to H_2O_2. The barrier (MP4SDTQ/6-31G*//HF/6-31G*) for oxidation of ammonia by methyl hydroperoxide (**TS-6c**, Figure 9b) is 53.5 kcal/mol above that of its isolated reactants. It should be noted that in the absence of optimization at a correlated level the barrier for the 1,2-hydrogen shift is lower than the oxygen-transfer barrier. By analogy to water oxide we suggest that this is also a two-step process and the barrier for oxygen transfer from intermediate methanol oxide is 7.9 kcal/mol. The transition structure is quite similar to that observed with water oxide as one might expect since the major electronic reorganization in both reactions is associated with changes in the O–O bond. It appears that water oxide can serve as an adequate model for theoretical studies of oxygen transfer from alkyl hydrogen peroxide. We further suggest that
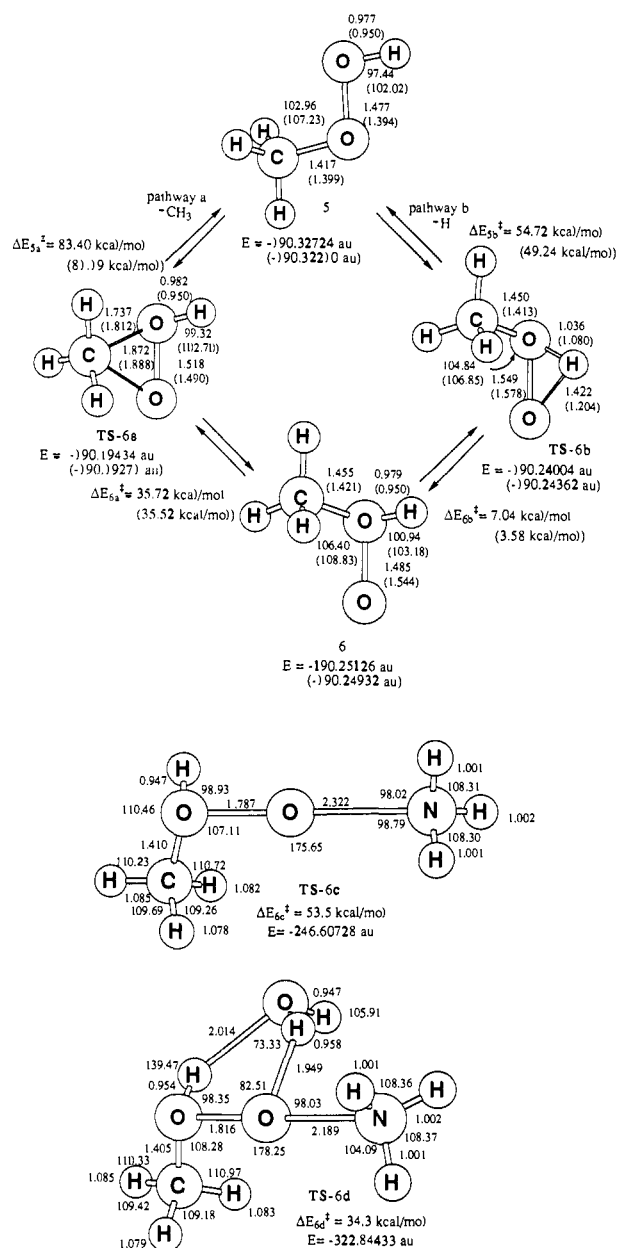
Figure 9. (a) A comparison of the 1,2-hydrogen and 1,2-methyl shifts for the formation of methanol oxide. (Optimized transition structures at the MP2/6-31G* level, HF/6-31G* geometry is in parentheses.) (MP4SDTQ/6-31G*//MP2/6-31G* in kcal/mol (no ZPE), MP4SDTQ/6-31G*//HF/6-31G* values in parentheses.) (b) Optimized transition structures for $CH_3OOH + NH_3 \rightarrow CH_3OH + H_3NO$ with and without water catalysis. (Optimized transition structures at the HF/6-31G* level, MP4SDTQ/6-31G*//HF/6-31G* in kcal/mol (no ZPE).)

a larger alkyl group such as *tert*-butyl would not have an appreciable effect on the energetics of oxygen transfer in the absence of solvent effects. As noted below even a single water molecule significantly lowers the oxidation barrier for reactions with CH_3OOH.

Water Catalysis in Oxygen Atom Transfer. The magnitudes of the above gas-phase barriers are simply too high to be compatible with those of observed oxygen-transfer chemistry in solution. Such reactions are typically carried out in aqueous solution or in the presence of protic solvent. The role of solvation becomes eminently clear when H_2O_2 and water oxide are stabilized by a molecule of water. The calculated decrease in energy for the $H_2O_2 \cdot H_2O$ (7, Figure 10) stationary point is 9.7 kcal/mol while that for $H_2OO \cdot H_2O$ (8) is 21.9 kcal/mol (MP4SDTQ/6-31G*//MP2/6-31G*).[13] This stabilization energy is far in excess

Table V. Barriers Relative to Isolated Reactants for $NH_3 + H_2O_2 + n(H_2O)$ [$n = 0, 1, 2$][a]

	HP/6-31G*// HF/6-31G*	MP4/6-31G*// HF/6-31G*	MP2/6-31G*// MP2/6-31G*	MP4/6-31G*// MP2/6-31G*
TS-3 ($n = 0$)	41.7	52.1[b]	57.5	51.3[c]
TS-9 ($n = 1$)	28.8	31.8	34.6	29.4 (39.1)[d]
TS-10 ($n = 2$)	18.5	14.9	16.0	11.2 (33.1)[e]

[a] Relative energies in kcal/mol (no ZPE); MP4SDTQ calculations are frozen core and MP2 calculations are full. [b] Barrier relative to $H_2O_2 \cdot NH_3$ linear complex is 62.9 kcal/mol. [c] Barrier relative to water oxide + NH_3 cyclic complex is 24.3 kcal/mol. [d] Barrier relative to $H_2O_2 \cdot H_2O$ complex 7 and isolated NH_3. [e] Barrier relative to $H_2O_2 \cdot H_2O$ complex 9 and isolated NH_3.

of what we had anticipated on the basis of a typical hydrogen bond[13] and reflects the dipolar nature of the O–O bond in water oxide and the basicity of the oxenoid oxygen. The cyclic hydrogen-bonded complex **8** is 11.2 kcal/mol more stable than a more conventional linear complex of H_2OO and water (H_2O-O⋯HOH).

Although the barriers (Table III) for a concerted S_N2 displacement by ammonia on hydrogen peroxide (TS-3) are surprisingly high (51.3 kcal/mol), a direct displacement of OH^- from H_2O_2 without a 1,2-hydrogen shift would afford OH^- and H_3NOH^+ that is 198.2 kcal/mol (HF/6-31G*) above the energy of the reactants in the gas phase. Solvation of a hydroxide ion by one water molecule affording bihydroxide ion ($H_3O_2^-$) is accompanied by only 35.2 kcal/mol (HF/6-31G*) of stabilization. Consequently, the gas-phase oxidation of NH_3 must be accompanied by a 1,2-hydrogen migration that is complete prior to N–O bond making in the transition state. The overall oxygen transfer is therefore very likely a two-step process involving S_N2 attack by ammonia on water oxide.

The origin of the barrier for a 1,2-hydrogen shift across an O–O bond may be attributed in part to the fact that the rearrangement is a 4-electron process involving a filled in-plane π^*-type O–O orbital. The barrier for formation of water oxide is 56.0 kcal/mol while a concerted 1,2-rearrangement of H_2O_2 hydrogen bonded to one water molecule (TS-7) still exhibits a barrier of 44.1 kcal/mol (MP4SDTQ/6-31G*//HF/6-31G*) from the $H_2O_2 \cdot H_2O$ complex (Figure 10). In principle, a water molecule serving as a catalyst can circumvent this problem in H_2O_2 or in an alkyl hydrogen peroxide by accepting a proton from the distal peroxide oxygen and transferring one of its hydrogens to the proximal oxygen (α-oxygen of the ROOH) effecting a formal 1,4-hydrogen shift as depicted in TS-8. The 1,4-shift barrier is 38.2 kcal/mol while the barrier for the reverse process is only 1.4 kcal/mol.

The reaction path for S_N2 displacement by NH_3 on hydrogen-bonded water oxide (TS-9) was followed in internal coordinates[8d] and leads from TS-9 back toward solvated water oxide and ammonia, supporting the proposed protonation–deprotonation pathway. Solvated water oxide, **8** (Figure 10), is stabilized by 21.6 kcal/mol relative to H_2OO and H_2O. We also searched the potential energy surface for an ionic transition structure involving oxygen transfer prior to 1,2-hydrogen shift. In an attempt to locate such a TS, we constrained the O_1H_1 bond distance at 1.09 Å and re-optimized the remaining parameters. This constrained structure (TS-9a) that is very close to a saddle point lies 29.0 kcal/mol (HF/6-31G*) above the first-order saddle point TS-9. Release of the O_1H_1 bond constraint immediately resulted in hydrogen transfer (H_1) to O_3 affording TS-9 with the attendant decrease in energy. We were able to locate a saddle point,[14] albeit with great difficulty, when the transition structure was optimized at MP2/6-31G*. In TS-9b the leaving group is a hydroxide ion complexed to a water molecule (bihydroxide ion), and this fragment is loosely hydrogen bonded to the developing NH_3OH^+ moiety. This involves the making and breaking of three oxygen–hydrogen bonds, and these stretching motions are highly

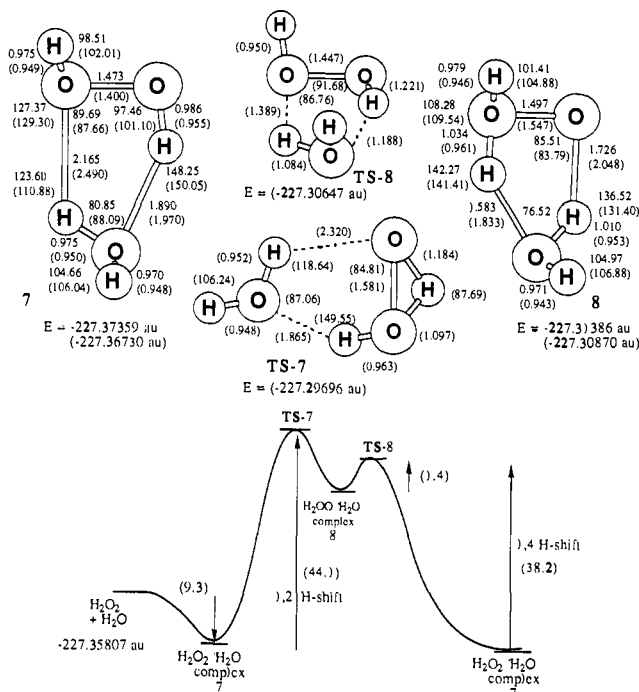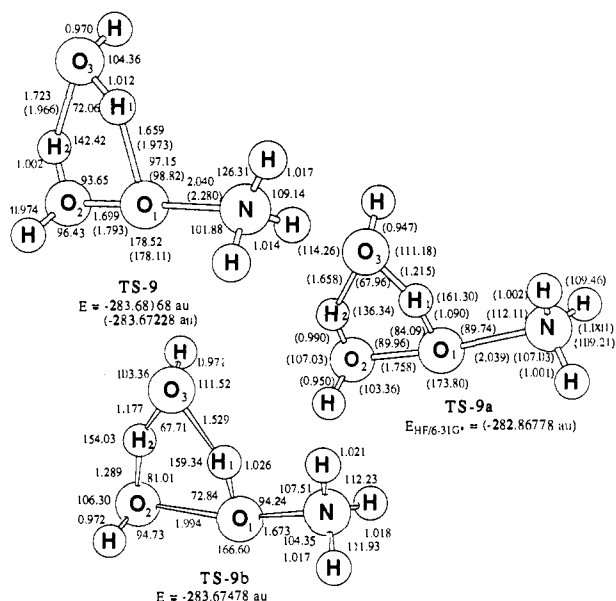(13) Hydrogen-bonded structures with one and two waters afford stabilization energies of 20.6 and 40.8 kcal/mol at the MP4STDQ/6-31G*// HF/6-31G* level of theory. The hydrogen bonds are typically much shorter with the MP2 calculations. The O–H bond distance in water dimer is 2.03 Å. At a higher level of theory the enthalpy for the formation of water dimer at the MP4SDTQ/6-31G*//HF/6-31G* and MP4/6-31+G(2d,2p) levels is −7.4 and −3.6 kcal/mol, respectively: Del Bene, J. E. *J. Phys. Chem.* **1988**, *92*, 2874. At the former level the hydrogen-bonding stabilization of H_2O_2 and H_2O is 9.3 kcal/mol.

Figure 10. Hydrogen peroxide (**7**) and water oxide (**8**) hydrogen bonded to a mole of water and a comparison of the transition structures for a 1,2-hydrogen shift (TS-7) versus a 1,4-hydrogen shift (TS-8) for H_2O_2 hydrogen bonded to a H_2O molecule. (Optimized transition structures at the MP2/6-31G* level, HF/6-31G* geometry in parentheses; MP4SDTQ/6-31G*//MP2/6-31G* relative energies in kcal/mol (no ZPE), MP4SDTQ/6-31G*//HF/6-31G* values in parentheses.)

coupled with the S_N2 component of the transition vector making it more difficult to locate the stationary point. We found TS-9b to be only 4.3 kcal/mol higher in energy than TS-9 where the hydrogen shift occurs prior to the transition state. Although the energies of these two transition structures are comparable, that is where the similarities end. For example, TS-9 resembles ammonia oxide with a negative charge (−0.27) on O_1 and a positively charged (0.20) water molecule (H_2O_2H) as a leaving group. Ionic TS-9b is essentially protonated ammonia oxide with a positive charge (0.22) on the $O_1–H_1$ fragment complexed to bihydroxide ion (HO_2^-⋯H_2O_3H) with a negative charge (−0.61) on the hydroxide ion ($H–O_2$) leaving group. The most striking difference, however, is in the extent of electron transfer from the NH_3 fragment in TS-9 (0.08 electrons) and TS-9b (0.47 electron) which is reflected in a markedly different O–O bond distance. These transition structures are sufficiently close in energy to suggest that both pathways a feasible, and that oxygen atom transfer can occur prior to or after the hydrogen shift. The significant point that emerges is that *some form of catalysis is essential in order to effect oxygen atom transfer from the hydroperoxide moiety* and the actual pathway can be markedly influenced by the nature of the solvent.

The overall barrier from isolated reactants for oxidation of ammonia by methyl hydrogen peroxide (Figure 9b) is also reduced from 53.5 to 34.3 kcal/mol by the action of one molecule of water catalyst (TS-6d). The geometry of the transition state clearly reflects the two-step nature of the oxidation process and resembles solvated methanol oxide involved in an S_N2 process with :NH_3. Transition-state changes relative to the comparable process with

6010 *J. Am. Chem. Soc., Vol. 113, No. 16, 1991*

Bach et al.

Figure 11. Transition structure (TS-9) for oxygen atom transfer from H_2OO to NH_3 with one water. (Optimized geometry at the MP2/6-31G* level, HF/6-31G* geometry in parentheses; MP4SDTQ/6-31G*//MP2/6-31G* relative energies in kcal/mol (no ZPE), MP4SDTQ/6-31G*//HF/6-31G* values in parentheses.) Optimized geometry (HF/6-31G* second-order saddle point) for oxygen atom transfer from H_2O_2 to NH_3 with one water where the O_1–H_1 bond is necessarily constrained (1.09 Å).

water oxide are unexceptional. Inclusion of electron correlation when studying a 1,2-hydrogen shift for methyl hydrogen peroxide led to the prediction of a stable methanol oxide. The same theoretical treatment of the water-catalyzed reaction would undoubtedly lead to shorter hydrogen bonds in the transition structure.

Although a remarkable decrease in the 1,2-hydrogen shift barrier in H_2O_2 results from catalysis by one water, a barrier for oxygen transfer of 29.4 kcal/mol relative to the isolated reactants (TS-8, Table V) would still be much too high to be commensurate with a reagent with such a high oxygen donation potential. The reduction in the barrier in protic media must reflect both the amelioration of the 1,2-hydrogen shift barrier and a decrease in electron density at the "electrophilic" oxygen; however, the greatest effect comes from stabilization of water oxide itself by hydrogen bonding. Although H_2O_2 hydrogen bonded to two water molecules affording the cyclic structure 9 is stabilized by 21.9 kcal/mol, the hydrogen-bonded cyclic array, involving water oxide, is 42.7 kcal/mol lower in energy than its separated entities, and only 7.0 kcal/mol above the energy of isolated H_2O_2 plus two water molecules. We therefore employed a second water molecule (TS-10, Figure 12) and the barrier for oxygen atom transfer from hydrogen peroxide and two isolated water molecules dropped to 11.2 kcal/mol for an overall decrease in activation energy of 40.1 kcal/mol. More significantly, the barrier for oxygen transfer (TS-10) from solvated water oxide 10 is only 4.2 kcal/mol. Such a dramatic energy decrease is reflective of the unusual reactivity of the water oxide functionality. The effect of 0, 1, and 2 molecules of solvent water on the barrier height for oxygen transfer is summarized in Figure 13.

Although there is no ambiguity in following the reaction path in internal coordinates from TS-3 back to its reactants, water oxide and ammonia, the geometric changes in TS-10 that would distinguish a dihydrated H_2O_2 (9) from $H_2OO·2H_2O$ (10) are more subtle. In the latter case the two O–H bonds on O_2 in water oxide should remain essentially unchanged. The reaction path was followed[8d] from TS-10 down toward reactants and products. The results indicate that TS-10 is connected to a structure resembling 10 in the reactant side while the product side is consistent with an S_N2 displacement on 10 forming the N-oxide and 3 mol of water (Figure 14).
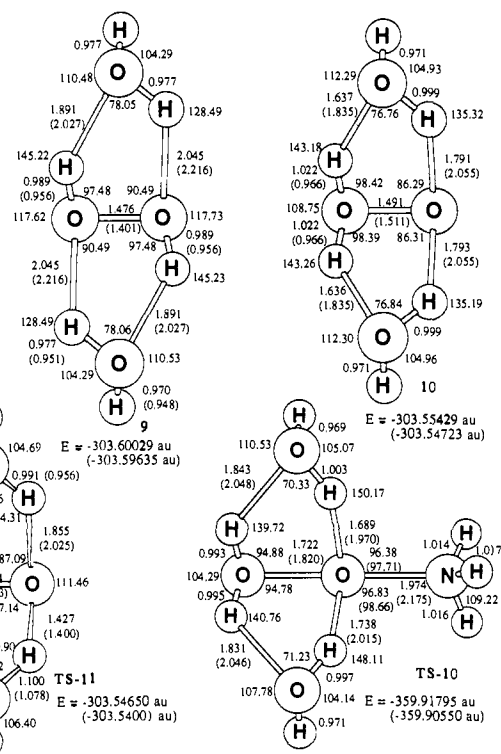

Figure 12. Optimized geometries for H_2O_2 (9), H_2OO (10), and the transition-state geometries for oxygen atom transfer from H_2OO to NH_3 with two waters (TS-10) and the 1,4-hydrogen shift in H_2O_2 hydrogen bonded to a second H_2O (TS-11). (Optimized structures at the MP2/6-31G* level, HF/6-31G* geometry in parentheses; MP4SDTQ/6-31G*//MP2/6-31G* in kcal/mol (no ZPE), MP4SDTQ/6-31G*//HF/6-31G* values in parentheses.)
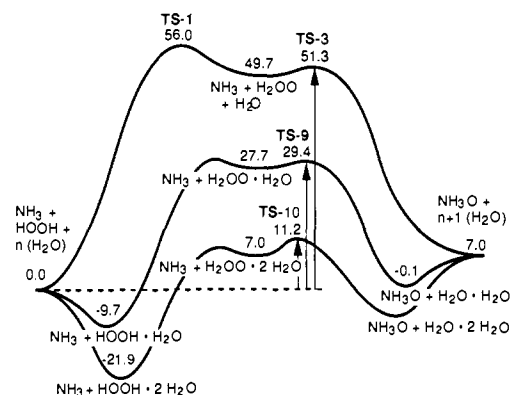
Figure 13. Activation barriers for oxygen atom transfer from H_2O_2 to NH_3 catalyzed by zero, one, or two molecules of water (MP4SDQ/6-31G*//MP2/6-31G* in kcal/mol without ZPE).

The present study strongly suggests that a simple S_N2 displacement (eq 1) cannot account for the oxygen donation potential of either H_2O_2 or ROOH since it does not accommodate the energy requirements for the 1,2-hydrogen shift. *An oxygen transfer process such as that depicted in TS-10 requires an oxenoid oxygen atom and a neutral leaving group.* A concerted 1,4-hydrogen shift in hydrogen peroxide stabilized by a second molecule of water (TS-11) still has a barrier of (9 to 10) 33.8 kcal/mol. The solvated water oxide 10 is 28.9 kcal/mol higher in energy than $H_2O_2·2H_2O$ (9) and its barrier for reversion to 9 is only 4.9 kcal/mol. This barrier is only 0.7 kcal/mol higher than that for oxygen transfer in TS-10 when both barriers are calculated relative to H_2O_2 complexed to two water molecules as in 9. The hydrogen transfer can be more easily achieved by simple protonation–deprotonation circumventing the more energetically demanding 1,2-hydrogen shift. Hence, the potentially exorbitant barrier for this overall process may be abated by the stabilizing influence of one or more water molecules.[14] The data in the
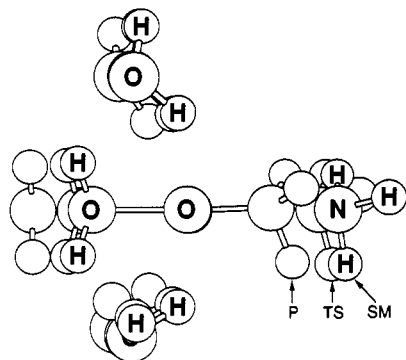
Figure 14. Three points along the reaction path obtained by the reaction path following algorithm at the HF/6-31G* level of theory: SM, starting materials (structure **10**); TS, transition state (**TS-10**); P, along the path toward the products (ammonia oxide + 3 molecules of water, hydrogen bonded).

present study also strongly suggest that a structure resembling **TS-10** is involved in a great many reactions of hydrogen peroxide in protic solvent where a proton relay is possible.

Acid Catalysis in Oxygen Atom Transfer. The role of solvation and the need for a neutral leaving group in these S_N2-type displacements resulting in oxygen transfer have been amply demonstrated. The trends noted in the activation barriers clearly suggest that oxygen transfer would be more facile in bulk solvent than in the gas phase. A cyclic activated complex utilizing water or a protic solvent has been suggested earlier on the basis of kinetic studies on the oxidation of sulfides by *tert*-butyl hydroperoxide (**11**).[15] In the absence of protic solvent a second molecule of alkyl hydrogen peroxide apparently dimerizes in solution and plays the role of protic solvent in the hydrogen shift, **11a**. Our data are consistent with this suggestion that has been amply verified experimentally by a change in the kinetic order from one to two in peroxide.[15]
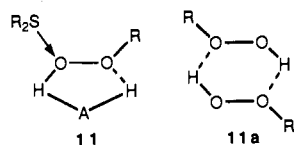
At the outset we examined the mechanism for oxygen transfer from H_2O_2 to the neutral nucleophilic ammonia. An ionic mechanism involving hydroxide ion as a leaving group was avoided by hydrogen transfer to form water oxide prior to the oxygen-transfer step. At the other end of this mechanistic spectrum, a fully protonated hydrogen peroxide would provide the neutral leaving group water. The ultimate test of this requirement would be to examine the barrier for oxygen transfer from protonated H_2O_2 (**12**) to NH_3 as shown in **TS-12**. This reaction affording NH_3OH^+ and H_2O has a first-order transition structure that lies 29.4 kcal/mol *below* its reactants. Because proton transfer from $H_3O_2^+$ to NH_3 is exothermic by 50.0 kcal/mol, we did not attempt to locate the complex that precedes **TS-12** on the reaction path. In this reaction the proton is clearly transferred from NH_3OH^+ after the rate-limiting oxygen-transfer step. The water-catalyzed reactions discussed above lie between these two extremes. It would not be unreasonable to expect a proton transfer to H_2O_2 from bulk proton solvent, followed by facile oxygen atom transfer to NH_3 and proton transfer from NH_3OH^+.

In summary, we have established the importance of electron correlation in the 1,2-hydrogen shift in H_2O_2 and in the gas-phase
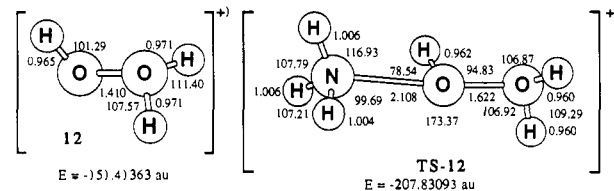
Figure 15. Byhydroxide cation (**12**) and its transition state for oxygen atom transfer with ammonia (**TS-12**). (Optimized geometries at HF/6-31G* level, energies at MP4/6-31G*.)

oxygen transfer from hydrogen peroxide to ammonia and ethylene. The "electrophilic" oxygen atom has a full octet of electrons around oxygen in the transition state and the leaving group is essentially neutral water. Although water oxide or an alcohol oxide may have only a fleeting existence in the gas phase, they are viable transient entities in protic solvent. We have also provided data that suggest that ammonia oxide is a relatively poor oxygen donor as a result of electron repulsion and a relatively strong N–O bond, in good agreement with experimental data on tertiary amine oxides.[17] The reactivity of these oxygen-donor reagents is a consequence of a σ bond that, upon nucleophilic attack, elongates readily and yields a relatively low energy empty σ^* orbital to serve as an electrophile. Any mechanism involving oxygen atom transfer from the hydroperoxide functional group must accommodate the energetic requirements for the 1,2-hydrogen shift affording an oxenoid intermediate. We also suggest that our data[4b] have far-reaching implications in the area of flavin-mediated hydroxylation[16] where the flavin 4α-hydroperoxide has been suggested as the key intermediate that serves either as the oxygen donor or its immediate precursor. The simple mechanism involving oxygen atom transfer with a simultaneous 1,2-hydrogen shift as exemplified in eq 1 would have an activation barrier far in excess of that compatible with an oxygen donor capable of aromatic hydroxylation. Whether oxygen is donated from the simplest of donors such as H_2O_2 or more complex systems such as the 4α-flavin hydroperoxide, a means of effecting a formal 1,2-hydrogen transfer affording an oxy–oxonium ion intermediate resembling a solvated water oxide (or alcohol oxide) must precede the oxygen-transfer step in order for the activation barriers to be commensurate with those typically observed in the laboratory. Alternatively, in an ionic process solvent participation is required in order to stabilize the departing oxyanion resulting from heterolytic O–O bond cleavage. Thus, oxygen atom transfer from the hydroperoxide functional group occurs by a distinctly different mechanism from oxidation by a percarboxylic acid where a relatively stable carboxylate anion is ideally poised to accept a 1,4 migrating hydrogen *after the barrier is crossed*.[18] Since our calculations to date have involved only two water molecules, prudence would dictate that more highly solvated concerted or ionic mechanisms resembling **TS-9b** should not be totally excluded. We do advocate that the mechanisms involving solvent assistance described above should be given serious consideration by the experimentalist.

(14) Transition structure **9b** converged with the requisite single negative eigenvalue in the approximate Hessian used in the geometry optimization. Verification that this is indeed a first-order saddle point would involve calculation of the full Hessian at the MP2 level which is currently beyond our means.

(15) For a discussion of solvent-assisted proton transfer in alkyl hydrogen peroxides see: (a) Dankleff, M. A. P.; Ruggero, C.; Edwards, J. O.; Pyun, H. Y. *J. Am. Chem. Soc.* **1968**, *90*, 3209. (b) Swern, D. *Organic Peroxides*; Wiley-Interscience: New York, 1971; Vol. II, pp 73 and 74.

(16) (a) Walsh, C. In *Flavins and Flavoproteins*; Vincent, M., Williams, C. H., Eds.; Elsevier/North Holland: Amsterdam, 1981; pp 121–132. (b) Ballou, D. P. *Ibid.* **1982**; pp 301–310. (c) Bruice, T. C. *Ibid.* **1982**; pp 265–277. (d) Wierenga, R. K.; Kalk, K. H.; van der Laan, J. M.; Drenth, J.; Hofsteenge, J.; Weijer, W. J.; Jekel, P. A.; Beintema, J. J.; Muller, F.; van Berkel, W. J. *Ibid.* **1982**; pp 11–18.

(17) (a) Van Rheenen, V.; Kell, R. C.; Cha, D. F. *Tetrahedron Lett.* **1976**, 1973. (b) Wai, J. S. M.; Markó, I.; Svendsen, J. S.; Finn, M. C.; Jacobsen, E. N.; Sharpless, K. B. *J. Am. Chem. Soc.* **1989**, *111*, 1123.

(18) Bach, R. D.; Owensby, A. L.; Gonzalez, C.; Schlegel, H. B.; McDouall, J. J. W. *J. Am. Chem. Soc.* **1991**, *113*, 2338.